BB

cea

DAPNIA

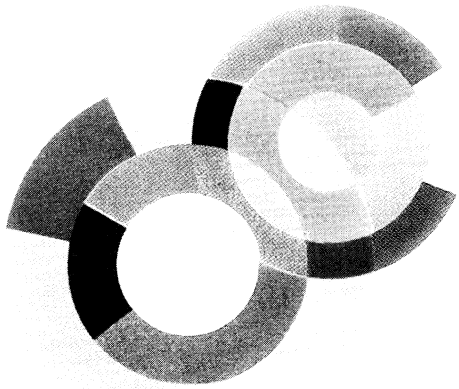

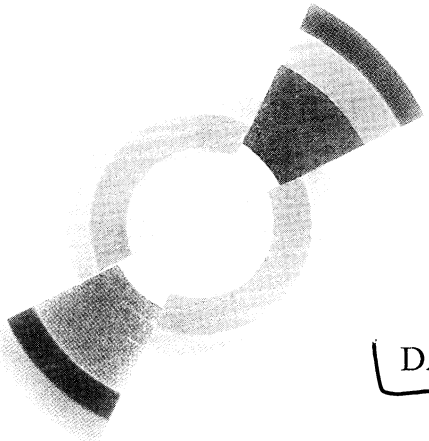

DAPNIA-05-32 03/2005

Directed and elliptic flow in $^{197}Au+^{197}Au$ at intermediate energies

J. Lukasik et al
(J.L. Charvet, R. Dayras,
R. Legrain, L. Nalpas, C. Volant)

Physics Letters B 608 (2005) 223-230

Département d'**A**strophysique, de Physique des **P**articules, de Physique **N**ucléaire et de l'**I**nstrumentation **A**ssociée

DSM/DAPNIA, CEA/Saclay F - 91191 Gif-sur-Yvette Cédex
Tél : (1) 69 08 24 02 Fax : (1) 69 08 99 89
http : //www-dapnia.cea.fr

Available online at www.sciencedirect.com
SCIENCE DIRECT®
PHYSICS LETTERS B
ELSEVIER
Physics Letters B 608 (2005) 223–230
www.elsevier.com/locate/physletb

Directed and elliptic flow in ^{197}Au + ^{197}Au at intermediate energies

INDRA Collaboration, ALADIN Collaboration

J. Łukasik [a,j], G. Auger [b], M.L. Begemann-Blaich [a], N. Bellaize [d], R. Bittiger [a], F. Bocage [d], B. Borderie [c], R. Bougault [d], B. Bouriquet [b], J.L. Charvet [e], A. Chbihi [b], R. Dayras [e], D. Durand [d], J.D. Frankland [b], E. Galichet [c,k], D. Gourio [a], D. Guinet [f], S. Hudan [b], P. Lautesse [f], F. Lavaud [c], A. Le Fèvre [a], R. Legrain [e,✠], O. Lopez [d], U. Lynen [a], W.F.J. Müller [a], L. Nalpas [e], H. Orth [a], E. Plagnol [c], E. Rosato [g], A. Saija [h], C. Schwarz [a], C. Sfienti [a], B. Tamain [d], W. Trautmann [a], A. Trzciński [i], K. Turzó [a], E. Vient [d], M. Vigilante [g], C. Volant [e], B. Zwiegliński [i]

[a] *Gesellschaft für Schwerionenforschung mbH, D-64291 Darmstadt, Germany*
[b] *GANIL, CEA et IN2P3-CNRS, F-14076 Caen, France*
[c] *Institut de Physique Nucléaire, IN2P3-CNRS et Université, F-91406 Orsay, France*
[d] *LPC, IN2P3-CNRS/ENSICAEN et Université, F-14050 Caen, France*
[e] *DAPNIA/SPhN, CEA/Saclay, F-91191 Gif-sur-Yvette, France*
[f] *Institut de Physique Nucléaire, IN2P3-CNRS et Université, F-69622 Villeurbanne, France*
[g] *Dipartimento di Scienze Fisiche e Sezione INFN, Università di Federico II, I-80126 Napoli, Italy*
[h] *Dipartimento di Fisica dell'Università and INFN, I-95129 Catania, Italy*
[i] *A. Soltan Institute for Nuclear Studies, PL-00681 Warsaw, Poland*
[j] *Institute of Nuclear Physics, PL-31342 Kraków, Poland*
[k] *Conservatoire National des Arts et Métiers, F-75141 Paris, France*

Received 21 October 2004; received in revised form 7 December 2004; accepted 22 December 2004

Available online 5 January 2005

Editor: V. Metag

Abstract

Directed and elliptic flow for the ^{197}Au + ^{197}Au system at incident energies between 40 and 150 MeV per nucleon has been measured using the INDRA 4π multi-detector. For semi-central collisions, the elliptic flow of $Z \leqslant 2$ particles switches from in-plane to out-of-plane enhancement at around 100 MeV per nucleon, in good agreement with the result reported by the

E-mail address: j.lukasik@gsi.de (J. Łukasik).
✠ Deceased.

0370-2693/$ – see front matter
doi:10.1016/j.physletb.2004.12.076

FOPI Collaboration. The directed flow changes sign at a bombarding energy between 50 and 60 MeV per nucleon and remains negative at lower energies. The conditions for the appearance and possible origins of the observed antiflow are discussed.

PACS: 25.70.Mn; 25.70.Pq; 25.40.Sc

Keywords: Symmetric heavy ion collision; Squeeze-out; Directed flow; Elliptic flow

Considerable progress has been made recently in determining the equation of state of nuclear matter from heavy-ion reaction data [1,2]. A prominent role among the available observables is played by the collective flow as it is most directly connected to the dynamical evolution of the reaction system, including the momentum dependence of nuclear interactions and in-medium effects (for reviews see [3,4]). Very significant constraints on the possible range of interaction parameters have been derived from transverse and elliptic flow variables [2].

For ^{197}Au + ^{197}Au collisions, the amplitudes of transverse and elliptic collective motion assume their maxima at bombarding energies of 300 to 400 MeV per nucleon. At these energies, the sign of the elliptic flow indicates a preference for emissions perpendicular to the reaction plane. The change-of-sign recently observed at ultra-relativistic energies has received particular interest as it reflects the increasing pressure buildup in the non-isotropic collision zone [5,6]. Toward the lower incident energies, the directed flow observables are presumed to be related to the competition of mean-field and nucleon–nucleon collision dynamics and their evolution with the bombarding energy [7–9]. Elliptic flow has been identified with the collective motion resulting from the rotation of the compound system or the expansion of the hot and compressed participant zone, possibly modified by the shadowing effect of the colder spectator matter [10–15]. Also here, at the intermediate energies, the transition energies at which the flow parameters change sign are particularly useful for the comparison with theory. Their correct prediction requires the cancellation of the competing momentum components which is highly sensitive to specific parameters of the theoretical description. A more technical advantage is the weak sensitivity of the transition energies to the resolution achieved in reconstructing the reaction plane.

In this Letter, we present results of the flow analysis applied to the data for ^{197}Au + ^{197}Au collisions at incident energies from 40 to 150 MeV per nucleon, collected with the 4π INDRA multi-detector [16] and with beams provided by the heavy-ion synchrotron SIS at GSI. With this energy range, the gap is bridged between existing excitation functions of collective motion in the relativistic and Fermi-energy domains. The transition from predominantly in-plane to out-of-plane emissions at about 100 MeV per nucleon, as reported by the FOPI Collaboration [15], is confirmed. Directed flow is found to change its sign at a bombarding energy below 60 MeV per nucleon [8], however with parameters that are found to depend strongly on the exact method applied and on the experimental acceptance.

Details of the experiment, including the identification and calibration procedures have been presented in Refs. [17,18] and references given therein. For impact parameter selection, the total transverse energy $E_\perp^{12}$ of light charged particles ($Z \leqslant 2$) was used as a sorting variable. The minimum-bias distributions of this quantity scale in proportion to the center-of-mass collision energy, which supports its usefulness as an indicator of the collision geometry. A maximum impact parameter $b_{\max} = 12$ fm $\pm$ 10% was deduced from the measured integrated beam intensity and the target thickness. It corresponds to the chosen trigger condition of at least 5 charged particles detected and, within errors, remains approximately constant over the covered range of bombarding energies. With this information, and assuming the monotonic relation [19] between the impact parameter and $E_\perp^{12}$, the data were sorted into six impact-parameter bins, each 2 fm wide and, altogether, covering the full range 0–12 fm. Particles of interest with $Z \leqslant 2$ were excluded from $E_\perp^{12}$ to reduce autocorrelations, a procedure found useful for peripheral collisions. It was further requested that at least 45% of the total charge of the system is detected, a condition used to reject peripheral events in which the projectile residue had escaped detection.

The kinetic-energy tensor, constructed from all identified charged particles, can be regarded as a

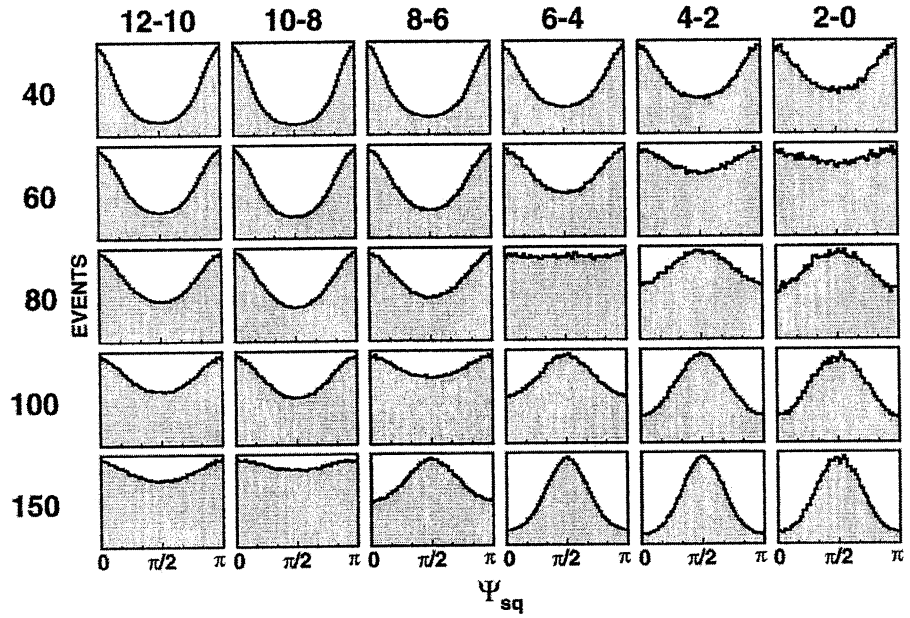

Fig. 1. Distributions of the squeeze angle Ψ_{sq} for incident energies from 40 to 150 MeV per nucleon (from top to bottom) and sorted into 2-fm-wide bins of the deduced impact parameter as indicated above each column of panels.

global observable characterizing the preferential directions of the particle and fragment emissions. The flow angle Θ_{flow} is defined as the angle between its largest eigenvector and the beam axis. Its distributions, analyzed with the weight $1/\sin\Theta_{flow}$ [20], are found to be mainly a function of centrality, with pronounced peaks at finite angles appearing at smaller impact parameters. The mean value increases from between 3° and 6° for peripheral to about 30° for central collisions. The excitation functions are fairly flat except for the most central collisions. For $b \leqslant 2$ fm, e.g., the weighted mean flow angle increases from about 15° to 40° for bombarding energies between 40 and 150 MeV per nucleon.

The squeeze angle Ψ_{sq}, defined as the angle between the middle eigenvector of the kinetic-energy tensor and the reaction plane [21], characterizes the preferential azimuthal directions of emission. The squeeze-angle distributions exhibit a clear trend as a function of incident energy and centrality (Fig. 1). The minima at $\pi/2$, observed at lower energies and more peripheral impact parameters, indicate predominantly in-plane emissions. Peaks at $\pi/2$, most strongly pronounced in the more central bins at the higher incident energies, correspond to a preference for azimuthal emissions perpendicular to the reaction plane, the so-called squeeze-out [21].

The curvature of the distributions has been analyzed using their standard deviation $\sigma(\Psi_{sq})$. The expression $\sigma(\Psi_{sq})/(\pi/\sqrt{12}) - 1$ is positive for concave distributions of Ψ_{sq}, negative for convex distributions, and zero for flat ones. The transition energies, E^{sq}_{tran}, identified by a change-of-sign of this variable, have been determined by a linear interpolation between bombarding energies. Linear extrapolations were used to obtain estimates for the very peripheral impact parameter bins.

The energies of the transition from predominantly in-plane to out-of-plane emissions are a strong function of the impact parameter (Fig. 2). They extend from 65 MeV per nucleon for central collisions up to about 200 MeV for the most peripheral collisions and exhibit an increasingly rapid rise toward the more peripheral impact parameters. Results obtained by representing the event with the kinetic-energy tensor or with a momentum tensor, i.e., without the weight factor $1/2m$, are identical at central impact parameters but diverge slightly in the peripheral bins.

The diagonalized tensors provide a global representation of the collective event properties. A much more

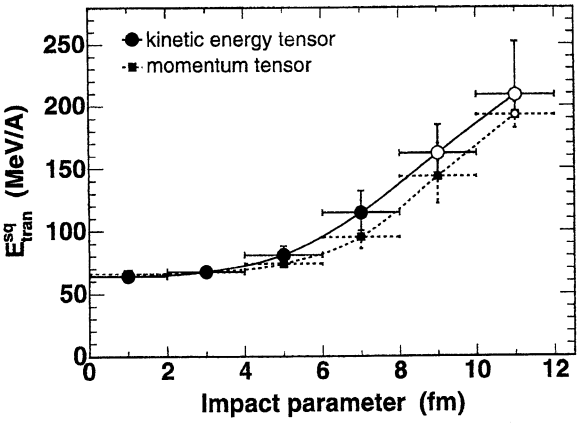

Fig. 2. In-plane to out-of-plane transition energies, E^{sq}_{tran}, determined from the curvatures of the squeeze-angle distributions, as a function of the impact parameter b. The full and empty symbols indicate interpolated and extrapolated values, respectively. The full (dashed) line connects results obtained from analyses with a kinetic-energy (momentum) tensor for the event description. The horizontal error bars represent the widths of the impact-parameter bins and the vertical errors result from the systematic uncertainty of b_{max}.

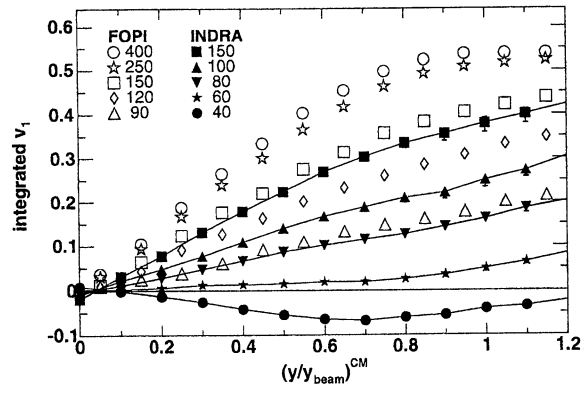

Fig. 3. Transverse-flow parameter v_1 for $Z = 2$ particles integrated over p_T as a function of scaled center-of-mass rapidity for mid-central collisions (2–5.3 fm). The open and filled symbols represent the FOPI [9] and the present data, respectively. The numbers in the legend indicate the beam energies per nucleon in MeV. The vertical error bars result from the systematic uncertainty of b_{max}.

detailed quantitative information can be obtained from the Fourier analysis of azimuthal distributions of the reaction products measured with respect to the reconstructed reaction plane and as a function of particle type, rapidity y and possibly the transverse momentum p_T. The first two coefficients, v_1 and v_2, of the Fourier expansion characterize the directed and elliptic flow, respectively [22–25]. The reaction plane has been determined by several methods, including the flow-tensor method [26], the flow Q-vector method [27], and the azimuthal-correlation method [28].

The rapidity dependence of the directed-flow parameter v_1 for $Z = 2$ particles, integrated over transverse momentum, is shown in Fig. 3. The present INDRA data are combined with the FOPI data [9], both measured for mid-central collisions with impact parameters of 2–5.3 fm and shown without corrections for the reaction plane dispersion. In the case of the INDRA data, the reaction plane has been reconstructed using the Q-vector method with the weights $\omega = p_z$, excluding the particle of interest ("1 plane per particle") and correcting for the effects of momentum conservation [29]. Corrections for the reaction plane dispersion are uncertain when the multiplicity is low. At 150 MeV per nucleon, the multiplicities are high, and correction factors for the v_1 parameter extracted from the FOPI and the INDRA data agree within a few percent. This indicates that the instrumental contribution to the uncertainty of the reaction plane reconstruction is similar for both detectors.

The slope of v_1 as a function of rapidity is seen to rise monotonically with energy over the full range of 40 to 400 MeV per nucleon which is covered by the two experiments. Good agreement is observed in the overlap region which, e.g., may be verified at the incident energy of 150 MeV per nucleon which was used in both experiments. The coefficient v_1 and its slope as a function of rapidity are practically zero at 60 MeV per nucleon and become even negative at 40 MeV per nucleon. This intriguing observation of a negative flow has already been reported for the lighter systems ^{40}Ar + ^{58}Ni, ^{58}Ni + ^{58}Ni, and ^{129}Xe + ^{nat}Sn, provided the 1-plane-per-particle method was used [30]. For these systems, a balance energy, E_{bal}, has been determined by associating it with the minima of the approximately parabolic excitation functions of the flow parameter which, in the cases of ^{40}Ar + ^{58}Ni and ^{58}Ni + ^{58}Ni, appeared at negative flow values. If the same parabolic scenario is adopted for the present case of ^{197}Au + ^{197}Au, the balance energy should fall below the observed zero-crossing of the slope dv_1/dy for which the value 54 ± 4 MeV per nucleon has been obtained from interpolation.

Values for the balance energy in ^{197}Au + ^{197}Au have previously been determined by extrapolating

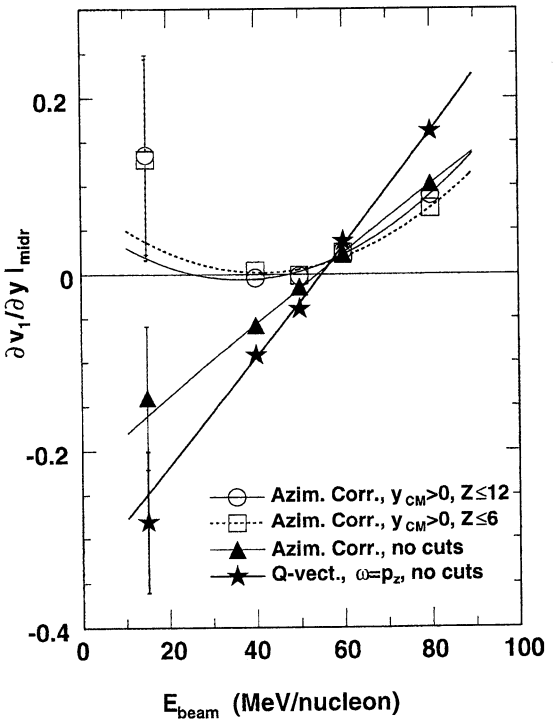

Fig. 4. Excitation functions of the mid-rapidity slopes of the v_1 parameter for $Z = 2$ particles and impact parameters 0–4 fm. The symbols correspond to the indicated methods and conditions used to define the reaction plane. The lines represent parabolic fits. The statistical errors, only shown for 15 MeV per nucleon, are smaller than the symbol size at other energies.

from higher energies [31–33], and also by searching for the minimum of flow [8]. The extrapolations yielded values between 47 and 56 MeV per nucleon with a moderate precision but, nevertheless, consistent with the zero-crossing at 54 ± 4 MeV per nucleon observed here. The excitation function of flow reported in Ref. [8] has a minimum at $E_{bal} = 42 \pm 4$ MeV per nucleon but the measured slopes were exclusively positive for products with $Z > 1$, which is contrary to the present data.

In order to identify the possible sources of the apparent disagreement between these two measurements, the present data has been subjected to similar thresholds and selection criteria as used in Ref. [8] and analyzed with the same azimuthal-correlation method of reaction-plane reconstruction [28], excluding the particle of interest. The flow is represented by the slopes dv_1/dy, determined by linear fits within the range of the scaled center-of-mass rapidity $-0.5 \leqslant y_{cm}/y_{cm}^{proj} \leqslant 0.5$. The results for $Z = 2$ are summarized in Fig. 4, including data for 15 MeV per nucleon from a small data sample primarily collected for calibration purposes.

With the conditions $Z \leqslant 12$ or $Z \leqslant 6$ for the reaction plane reconstruction, the parabolic excitation function of the flow parameter reported in Ref. [8] is qualitatively reproduced (open symbols in Fig. 4). The restriction to positive center-of-mass rapidities has been identified as causing the sizable negative offsets of v_1 at mid-rapidity in this data, without altering the slopes. The effect of the energy thresholds and angular acceptance cuts has been found to be negligible. Without the restriction to small charges, the minimum disappears, and the flow continues to decrease to more negative values, apparently down to bombarding energies as low as 15 MeV per nucleon. The Q-vector method of the reaction plane reconstruction with the weights $\omega = p_z$ yields larger absolute flow values. The larger weights assigned to the faster and heavier fragments may cause a better definition of the reaction plane [34]. Similar trends are also observed for heavier fragments ($Z = 3$–9).

The origin of the negative directed flow observed in the present data and the strong effects of the acceptance and selection criteria are illustrated in Fig. 5. The left column of panels shows contour plots of the in-plane transverse velocity versus the center-of-mass rapidity. For peripheral collisions at high incident energy (top panels) the deflections of the projectile and target, as represented by the three-dimensional Q-vector, are small. The Coulomb repulsion from the heavy residues leads to the apparent depression of helium yields near the entrance-channel rapidities of ± 0.28 and to maximum intensities at lower absolute rapidity, as discussed in Ref. [35]. The stronger deflection of mid-rapidity particles is evident from the rapid rise of v_1 with y_{cm} which, at $y_{cm} \approx 0.2$, starts to be modified by the effect of the projectile and target spectators. The resulting pattern appears similar to the two-component flow obtained in quantum-molecular-dynamics calculations for large impact parameters [36].

At 40 MeV per nucleon, and the same peripheral impact-parameters (middle panels of Fig. 5), the structure of v_1 as a function of y_{cm} is qualitatively the same as at 150 MeV per nucleon but compressed into a smaller range of absolute rapidity. In central collisions, at this energy, the distributions are even more

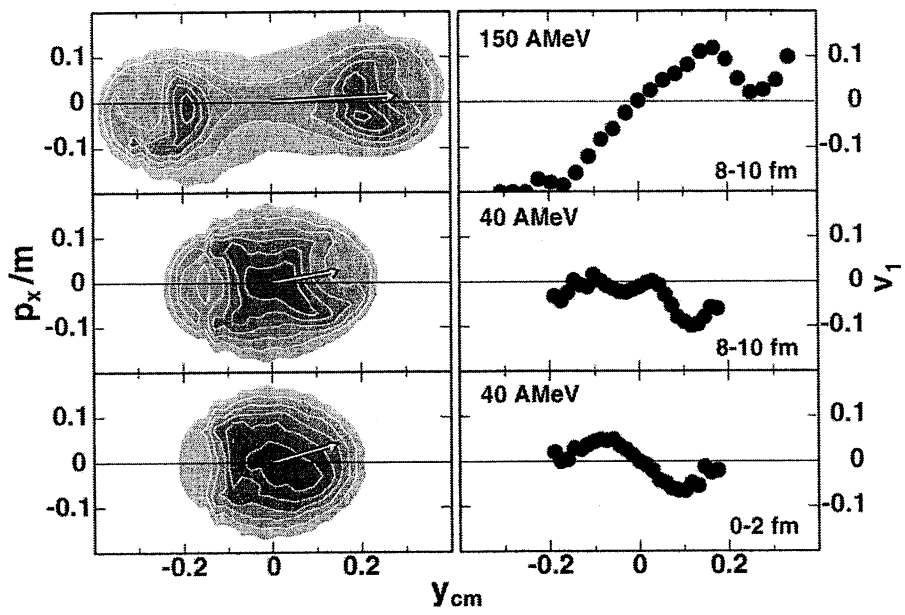

Fig. 5. Contour plots (in linear scale) of the in-plane component of the transverse velocity (p_x/m) versus the center-of-mass rapidity y_{cm} (left column) and the coefficient v_1 as a function of y_{cm} (right column) for $Z = 2$ particles and three selected cases of incident energy and impact parameter as indicated. The arrows represent the directions of the three-dimensional Q-vector.

compact (Fig. 5, bottom left). The flow vector indicates the mean transverse deflection of the forward-emitted part of the event. This concentration of mass and charge, apparently, causes the $Z = 2$ particles to be preferentially deflected to the opposite side. The resulting flow, evaluated around mid-rapidity, is negative (antiflow). Clearly, Q-vectors that do not contain the momenta of the heavier fragments causing this deflection or shadowing will have different directions, and the flow measured relative to them may appear positive.

The absolute sign of the deflection angle cannot be determined with the present methods. There is little doubt, however, that the positive flow above 60 MeV per nucleon is associated with an overall positive deflection as a result of the dominant nucleon–nucleon dynamics. Near and above the Coulomb barrier, positive deflection angles follow from the dominance of the Coulomb forces. The present observation of a negative flow below 60 MeV per nucleon may thus indeed indicate a transition toward predominantly negative-angle emissions for light products, as concluded in Ref. [8], but also consistent with polarization measurements for light fragments, even though for other reactions [37]. Thus, the commonly invoked picture of the attractive mean field globally balancing the repulsive effect of the collisions seems to be too simple here to explain the observed sign change of flow. The main difference, as compared to lighter reaction systems, is the enlarged Coulomb field which not only has a strong impact on the entrance and exit channel trajectories [36] but also manifests itself in large repulsion effects (larger so-called Coulomb rings).

The elliptic-flow parameter v_2 permits a detailed study of azimuthal emissions including their mass and p_T dependence, as reported for incident energies of 90 MeV per nucleon and higher in Ref. [15]. The present data set, due to a higher efficiency for fragments, also reveals a significant effect of the fragment charge. Over the range of atomic numbers $Z \leqslant 2$ to $Z = 9$, the transition energy E_{tran}, evaluated in the laboratory frame, decreases from about 100 to 65 MeV per nucleon. The restriction to light particles, on the other hand, permits a comparison with other data sets and an extension of the measured excitation function deeper into the relativistic regime.

The excitation function of the elliptic flow for $Z \leqslant 2$ particles, in the rotated reference frame and for semi-

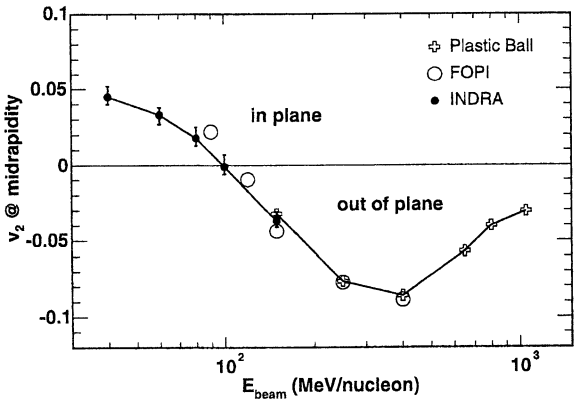

Fig. 6. Elliptic-flow parameter v_2 at mid-rapidity for $Z \leqslant 2$ particles from mid-central collisions, in the rotated reference frame. The dots, circles, and crosses represent the INDRA, the FOPI [15], and the Plastic Ball [21] data, respectively. The errors shown for the INDRA data are mainly systematic and caused by the uncertainty of b_{max}.

central collisions of 4–6 fm, as measured by the Plastic Ball [21],[1] the FOPI [15], and the INDRA Collaborations, is shown in Fig. 6. For this purpose, the present data has been analyzed with the same method as the Plastic Ball data, i.e., by using the kinetic-energy tensor for the reconstruction of the reaction plane and excluding the particle of interest. None of the three data sets were corrected for the reaction-plane dispersion. This correction is not expected to substantially alter the value of E_{tran} (cf. Ref. [15]) but will affect the values of v_2 at the lower energies at which the reaction plane is less well defined because of smaller particle and fragment multiplicities.

The observed agreement between the different experiments is very satisfactory. In particular, the value of the transition energy of around 100 MeV per nucleon, obtained by the FOPI Collaboration, is confirmed by the present data. Because of the Z dependence, it is approximately 20 MeV higher than the global transition energy derived from the kinetic-energy tensor for the same impact-parameter bin (Fig. 2). Together, the three data sets constitute a coherent systematics of v_2 which can be expected to serve as a valuable constraint for transport models.

[1] The MUL3 bin of the Plastic Ball data [21] is estimated to be approximately equivalent to the 4–6 fm bin of the INDRA and FOPI data [15].

In summary, the presented analysis of ^{197}Au + ^{197}Au collisions at intermediate energies extends the existing excitation functions of the flow parameters v_1 and v_2 from the relativistic regime down to the Fermi-energy regime. The observed transition from predominantly in-plane to out-of-plane emissions at about 100 MeV per nucleon for $Z \leqslant 2$ particles has been confirmed. The directed transverse flow changes its sign below 60 MeV per nucleon and becomes increasingly negative at lower bombarding energies. This antiflow and the absence of a parabolic excitation function of directed flow in ^{197}Au + ^{197}Au were shown to be connected to the large Coulomb effects in this reaction system.

Acknowledgements

The authors would like to thank A. Andronic and W. Reisdorf for making their data available and for valuable discussions. M.B. and C.Sc. acknowledge the financial support of the Deutsche Forschungsgemeinschaft under the Contract Nos. Be1634/1-1 and Schw510/2-1, respectively; D.Go. and C.Sf. acknowledge the receipt of Alexander-von-Humboldt fellowships. This work was supported by the European Community under contract ERBFMGECT950083.

References

[1] C. Fuchs, et al., Phys. Rev. Lett. 86 (2001) 1974.
[2] P. Danielewicz, et al., Science 298 (2002) 1592.
[3] W. Reisdorf, H.G. Ritter, Annu. Rev. Nucl. Part. Sci. 47 (1997) 663.
[4] N. Herrmann, et al., Annu. Rev. Nucl. Part. Sci. 49 (1999) 581.
[5] C. Adler, et al., Phys. Rev. Lett. 90 (2003) 032301.
[6] C. Adler, et al., Phys. Rev. Lett. 91 (2003) 182301.
[7] G.F. Bertsch, W.G. Lynch, M.B. Tsang, Phys. Lett. B 189 (1987) 384.
[8] D.J. Magestro, et al., Phys. Rev. C 61 (2000) 021602.
[9] A. Andronic, et al., Phys. Rev. C 64 (2001) 041604.
[10] W.K. Wilson, et al., Phys. Rev. C 41 (1990) 1881.
[11] M.B. Tsang, et al., Phys. Rev. C 47 (1992) 2717.
[12] R.A. Lacey, et al., Phys. Rev. Lett. 70 (1993) 1224.
[13] W.K. Wilson, et al., Phys. Rev. C 51 (1995) 3136.
[14] W.Q. Shen, et al., Phys. Rev. C 57 (1998) 1508.
[15] A. Andronic, et al., Nucl. Phys. A 679 (2001) 765.
[16] J. Pouthas, et al., Nucl. Instrum. Methods Phys. Res. A 357 (1995) 418.
[17] J. Łukasik, et al., Phys. Rev. C 66 (2002) 064606.

[18] A. Le Fèvre, et al., Nucl. Phys. A 735 (2004) 219.
[19] C. Cavata, et al., Phys. Rev. C 42 (1990) 1760.
[20] P. Danielewicz, M. Gyulassy, Phys. Lett. B 129 (1983) 283.
[21] H.H. Gutbrod, et al., Phys. Rev. C 42 (1990) 640.
[22] S. Voloshin, Y. Zhang, Z. Phys. C 70 (1996) 665.
[23] J.-Y. Ollitrault, nucl-ex/9711003.
[24] A.M. Poskanzer, S.A. Voloshin, Phys. Rev. C 58 (1998) 1671.
[25] N. Borghini, et al., Phys. Rev. C 66 (2002) 014901.
[26] M. Gyulassy, et al., Phys. Lett. B 110 (1982) 185.
[27] P. Danielewicz, G. Odyniec, Phys. Lett. B 157 (1985) 146.
[28] W.K. Wilson, et al., Phys. Rev. C 45 (1992) 738.
[29] C.A. Ogilvie, et al., Phys. Rev. C 40 (1989) 2592.
[30] D. Cussol, et al., Phys. Rev. C 65 (2002) 044604.
[31] W.M. Zhang, et al., Phys. Rev. C 42 (1990) 491.
[32] M.D. Partlan, et al., Phys. Rev. Lett. 75 (1995) 2100.
[33] P. Crochet, et al., Nucl. Phys. A 624 (1997) 755.
[34] C.A. Ogilvie, et al., Phys. Rev. C 40 (1989) 654.
[35] J. Łukasik, et al., Phys. Lett. B 566 (2003) 76.
[36] S. Soff, et al., Phys. Rev. C 51 (1995) 3320.
[37] M.B. Tsang, et al., Phys. Rev. Lett. 60 (1988) 1479.